AAC Accepted Manuscript Posted Online 15 October 2018
Antimicrob. Agents Chemother. doi:10.1128/AAC.01530-18

A pathway-directed screen for inhibitors of the bacterial cell elongation machinery

Jackson A. Buss[1], Vadim Baidin[2], Michael A. Welsh[1], Josué Flores-Kim[1], Hongbaek Cho[3], B. McKay Wood[1], Tsuyoshi Uehara[1], Suzanne Walker[1], Daniel Kahne[2], Thomas G. Bernhardt[1*]

[1]Department of Microbiology and Immunobiology
Harvard Medical School
Boston, MA 02115

[2]Department of Chemistry and Chemical Biology
Harvard University
Cambridge, MA 02138

[3]Department of Biological Sciences
Sungkyunkwan University
Suwon, Gyeonggi, Korea

[*]To whom correspondence should be addressed:

Thomas G. Bernhardt, Ph.D.
Harvard Medical School
Department of Microbiology and Immunobiology
Boston, Massachusetts 02115
e-mail: thomas_bernhardt@hms.harvard.edu

Running title: Screen for Rod system inhibitors

Keywords: cell wall synthesis, Rod system, MreB, peptidoglycan

ABSTRACT

New antibiotics are needed to combat the growing problem of resistant bacterial infections. An attractive avenue towards the discovery of such next generation therapies is to identify novel inhibitors of clinically validated targets like cell wall biogenesis. We have therefore developed a pathway-directed, whole-cell screen for small molecules that block the activity of the Rod system of *Escherichia coli.* This conserved multi-protein complex is required for cell elongation and the morphogenesis of rod-shaped bacteria. It is composed of cell wall synthases and membrane proteins of unknown function that are organized by filaments of the actin-like MreB protein. Our screen takes advantage of the conditional essentiality of the Rod system and the ability of the beta-lactam mecillinam to cause a toxic malfunctioning of the machinery. Rod system inhibitors can therefore be identified as molecules that promote growth in the presence of mecillinam under conditions permissive for the growth of Rod^- cells. A screen of ~690,000 identified 1,300 compounds active against *E. coli*. Pathway-directed screening of a majority of this subset of compounds for Rod inhibitors successfully identified eight analogs of the MreB-antagonist A22. Further characterization of the A22 analogs identified showed that their antibiotic activity under conditions where the Rod system is essential was strongly correlated with their ability to suppress mecillinam toxicity. This result combined with additional biological studies reinforce the notion that A22-like molecules are relatively specific for MreB and suggest that the lipoprotein transport factor LolA is unlikely to be a physiologically relevant target as previously proposed.

INTRODUCTION

New therapeutics are needed to overcome the growing problem of antibiotic resistant bacterial infections (1). A common approach for the identification of compounds with antibacterial activity is to screen large libraries of small molecules for potential antibiotic activity. Screens involving *in vitro* assays of purified enzymes have successfully identified inhibitors of essential bacterial targets (2). However, molecules discovered in this way often have limited activity on cells due to their inability to penetrate the bacterial envelope and/or due to their efficient efflux by resistance pumps (3). These issues are particularly acute for gram-negative bacteria, the outer membrane of which poses an especially difficult barrier for drugs to cross (4). Coupled with their efficient efflux systems that work synergistically with the outer membrane barrier, these organisms display a high level of intrinsic antibiotic resistance.

An alternative to target-directed *in vitro* screens are those performed on growing bacterial cells to identify molecules that block their replication. These screens have the advantage that positive hits are known to have antibacterial activity from the start. However, the disadvantages are that target identification is challenging and that many of the lethal molecules identified are non-specific poisons with metal-chelating, detergent-like, or redox active modes-of-action unsuitable for drug development (2, 3).

Pathway-directed, whole cell screens combine the practicality of screens performed on growing cells with a specificity that approaches that of an *in vitro* assay. As with traditional whole cell screens, this approach finds molecules with cellular activity. But, in this case, genetic logic is used in the design such that the screening readout identifies hit molecules with a mode-of-action that is likely limited to a particular biochemical pathway. Thus, the hits are enriched for compounds with specific, on-target activity. Previously published screens for

inhibitors that block wall teichoic acid (WTA) biogenesis in the gram-positive pathogen *Staphylococcus aureus* and a more recent application to discover inhibitors of lipopolysaccharide biogenesis in the gram-negative pathogen *Acinetobacter baumannii* are a classic example of the pathway-directed approach (5, 6).

The classic work that demonstrated the power of pathway-directed screening relied on the conditional essentiality of steps in wall teichoic acid (WTA) biogenesis (5). WTAs are anionic polymers attached to the peptidoglycan (PG) cell wall of gram-positive bacteria (7). They play important roles in the surface biology of these organisms and are essential for the virulence of *S. aureus* (8). WTA polymers are built on the undecaprenol-phosphate (Und-P) lipid carrier at the inner face of the cytoplasmic membrane. Once their synthesis is completed, they are transported across the membrane by the flippase TarGH and then attached to the PG layer by LCP enzymes (9, 10). Blocking the late steps of WTA synthesis is lethal due to the accumulation of lipid-linked precursor molecules that deplete the cell of Und-P carrier that is also needed for PG synthesis (11). However, this lethality can be suppressed by inactivating the first enzyme in the WTA biogenesis pathway, TarO, to prevent WTA precursor accumulation (11). Thus, a screen for molecules that kill wild-type cells but not those deleted for the *tarO* gene should identify inhibitors of late stage enzymes of the WTA synthesis pathway. Indeed, screens employing this logic successfully identified inhibitors that block the activity of the TarGH transporter (5).

In this report, we describe the development of a pathway-directed screen for compounds that disrupt the function of the cell elongation system of *Escherichia coli*. This PG biogenesis complex is called the Rod system (a.k.a. elongasome), and it consists of five integral membrane proteins organized by filaments of the actin-like MreB protein (12) (**Fig. 1A**). The

complex is normally essential for the growth of *E. coli* and other rod-shaped bacteria and is required for them to elongate their cell wall and maintain a capsule-like rod shape (13). All components of the Rod system are conserved and broadly distributed among bacteria, including the penicillin-binding protein called PBP2, a known beta-lactam target, and RodA, which was recently shown to function as a cell wall polymerase (14-16). Thus, the Rod system contains both proven and attractive new targets for therapeutic development.

As part of a broader program to identify new antibacterial agents, we screened a library of ~690,000 compounds for growth inhibitory activity against *E. coli*. We then counter-screened active molecules for activity against the Rod system using our pathway-directed readouts. Eight analogs of the MreB-antagonist A22 (17, 18) in the library were successfully identified, validating the effectiveness of our screening approach for identifying inhibitors of at least one component of the system. Further characterization of these inhibitors showed that their antibiotic activity under conditions where the Rod system is essential was strongly correlated with their ability to suppress mecillinam toxicity. This result combined with additional biological studies reinforce the notion that A22-like molecules are relatively specific for MreB and suggest that the lipoprotein transporter LolA is unlikely to be a physiologically relevant target of this scaffold.

Antimicrobial Agents and Chemotherapy

RESULTS

Rationale for the screen

The Rod system is normally essential (19). In *E. coli* and other rod-shaped bacteria, depletion of any component of the system causes cells to lose their rod-shape and develop into large spherical cells that eventually lyse (19). However, the lethality of Rod system inactivation can be suppressed in *E. coli* by moderate overproduction of the tubulin-like FtsZ protein (19) (**Fig. 1B**), filaments of which play a key role in the formation and activity of the cytokinetic ring apparatus (20). We use the term $FtsZ^{UP}$ to refer to cells producing extra FtsZ from the plasmid pTB63. $FtsZ^{UP}$ cells inactivated for components of the Rod system are viable and grow and divide as small spheres rather than rods. Although the mechanism by which increased FtsZ levels suppress Rod system essentiality is not known, the phenomenon has been useful for genetic analysis of the machinery and studies of the effects of antibiotics on its activity (21, 22).

Several years ago, we made the surprising observation that inhibition of the Rod system component PBP2 with a beta-lactam called mecillinam differs from genetic inactivation of the PBP2 encoding gene (22). This led us to discover that the PBP2-mecillinam complex causes the Rod system to malfunction and become toxic. Mecillinam-induced toxicity is caused by the inhibition of PG crosslinking by PBP2 while glycan chains continue being produced by RodA. Because the glycans cannot be crosslinked, they are rapidly degraded, resulting in a futile cycle of PG synthesis and breakdown by the Rod complex (22). Blocking PG synthesis by the Rod system in $FtsZ^{UP}$ cells prevents the futile cycle and suppresses mecillinam toxicity (**Fig. 1B**). Suppression can be achieved either by genetically inactivating Rod system components or by disrupting its activity with small molecules such as the MreB antagonist A22 (22). We therefore reasoned that other compounds that disrupt Rod system activity by targeting MreB or

other members of the complex (PBP2, MreC, MreD, RodA, RodZ) could be identified by screening for molecules that suppress the toxicity of mecillinam in an FtsZ^{UP} *E. coli* strain (**Fig. 1B**).

Screening for anti-Rod system compounds

Prior to screening for Rod inhibitors, 690,000 small molecules were tested for their ability to inhibit growth of an *E. coli* strain in which the *lptFG* genes were placed under control of the arabinose promoter and expressed at suboptimal levels (23). These genes encode components of the lipopolysaccharide (LPS) transport system such that the strain has a defective outer membrane permeability barrier, which was useful to maximize the number of lethal molecules identified. Compounds were assayed in duplicate. Endpoint absorbance (OD_{600}) readings for the test strain were measured following 23 hrs of growth in the presence of compounds (Fig. 2A). Hits were identified as those molecules causing a significant reduction (-2.5σ) in OD_{600} readings relative to the vehicle (DMSO) control (Fig. 2A). All commercially available hits along with some closely related analogs were purchased and assembled into a sub-library of 1,232 molecules to be used for identification of inhibitors for specific targets in gram-negative pathogens.

Using this sub-library as a starting point, the screen for Rod system inhibitors was performed in three steps: (i) screening the sub-library of lethal molecules for the ability to suppress mecillinam toxicity in FtsZ^{UP} cells, and (ii) using additional assays to test for on-target activity against the Rod system. We screened the sub-library for compounds capable of promoting growth of FtsZ^{UP} *E. coli* cells treated with mecillinam (2.5 µg/ml, 8 x MIC) (logic based on **Fig. 1B,** highlighted rows). A total of 72 compounds (5.7%) were found to suppress mecillinam toxicity (**Fig. 2B**), identifying them as potential Rod system inhibitors. However, prior genetic

studies indicate that the inactivation of over 60 genes in *E. coli* beyond those encoding Rod system components is capable of suppressing mecillinam toxicity (21). Thus, a range of different targets for the hit molecules identified in the Rod screen were possible. To identify true Rod system targeting molecules among the 72 mecillinam suppressors, we performed two additional assays. The first assay is based on the observation that the Rod system is non-essential in $FtsZ^{UP}$ cells (**Fig. 1B**). Therefore, the lethality of a molecule that targets the Rod system should be conditional and suppressed by elevated FtsZ levels. Of the 72 mecillinam suppressors, 44 compounds satisfied this screen and failed to block the growth of an $FtsZ^{UP}$ *E. coli* strain with a *tolC* deletion to weaken its outer membrane permeability barrier (**Fig. 2C**). Finally, the 44 hits from this screen were tested for their ability to alter cell shape. A total of eight compounds were identified that induced a shape change in target cells, consistent with the inhibition of Rod system function (**Fig. 1B, 3 and 4**).

Characterization of hit compounds

All eight of the hit compounds (**compounds 1-8, Fig. 4B**) are structurally similar to the known MreB antagonist A22 (**Fig. 4A**). A22 was discovered in a screen for inhibitors of chromosome partitioning (17) and was later found to inhibit the Rod system through a direct interaction with MreB (18, 24, 25). **Compound 1** most resembles A22 (**Fig. 4B**), and its anti-MreB activity was confirmed (**Table 1**). The remaining seven compounds (**compounds 2-8, Fig. 4B**) are S-triazine substituted analogs of the A22 scaffold reminiscent of MAC13243 (26) (**Fig. 4C**). This compound was initially identified as a growth inhibitor with a lethal activity that could be suppressed by overexpression of the *lolA* gene encoding an essential component of the lipoprotein transport machinery in gram-negative bacteria (26). However, it was subsequently found to undergo acid hydrolysis into an A22-like compound and to target MreB in *Pseudomonas aeruginosa* (**Fig. 4C**) (27, 28, 29). Consistent with these results, we found that

196 **compound 4** undergoes hydrolysis**,** and is active, whereas the related **compound 19** remains
197 intact and has drastically reduced A22-like cellular activity (**Table 1 and Fig. S1**). We therefore
198 infer that hit **compounds 2-8** (**Fig. 4B**) are all likely to require hydrolysis for anti-MreB activity.
199
200 **Efficacy of the screening procedure**
201 To better understand the relative effectiveness of the screen, we wanted to know how many
202 total A22-like molecules were in the original library and whether any potential hits were missed
203 during screening. To create a comprehensive list of all molecules resembling A22 in the initial
204 library used for the primary screen, we performed a similarity analysis with Pipeline Pilot from
205 SciTegic (30) using both an extended-connectivity bit string and a feature-connectivity bit string
206 (FCFP). We applied a loose threshold of 0.4-0.6 to avoid false negatives (31), and identified
207 154 analogs (**Table S1**). Of these 154 compounds, 51 inhibited growth (**Table S1**) and 14
208 were acquired for the bioactive sub-library (**Fig. 4B and C**). An additional four A22-like analogs
209 were purchased for assembly of the sub-library that were not present in the initial pool. Thus,
210 the bioactive library used for the mecillinam suppression screen contained 18 molecules with
211 similarity to A22 (**compounds 1-18, Fig. 4B and D**).
212
213 **Compounds 9-18** were not identified as having activity against the Rod system based on the
214 results of the sequential screening procedure (**Fig. 4D**). Consistent with prior SAR studies of
215 A22 (28, 29, 32-34), most of these molecules lack either the isothiourea or aryl halide moieties
216 important for bioactivity, and thus would not be predicted as screening hits. However,
217 **compounds 9-11** resembled A22 enough to warrant further investigation of their activity.
218 **Compound 9** effectively suppressed mecillinam toxicity, but did not induce cell rounding
219 (**Table 1**). **Compounds 10 and 11**, on the other hand, had weak activity that likely contributed
220 to their negative results in the screen. They required a concentration near or significantly

above the screening concentration to suppress mecillinam toxicity and induce cell rounding (**Table 1**). Based on the analysis of the A22-like hits from the screen and related negatives, we conclude that the screening procedure is effective at identifying MreB antagonists and does not suffer major issues with false negatives.

Relationship between MIC and mecillinam suppression activity of A22-like molecules

To determine the relationship between the MIC of A22-like molecules on wild-type cells and the concentration required for mecillinam suppression, we purchased **compounds 20-23** (**Fig. 4E)** and assayed their activities along with those of A22 and **compounds 1 and 11** (**Fig. 4B and D**). As expected based on prior studies of these molecules (28, 29, 32-34), they all killed wild-type *E. coli* and induced a rod-to-sphere shape change (**Table 1, Fig. S2**). With the exception of **compound 11**, which had weak activity, all of the molecules suppressed mecillinam toxicity with a minimal concentration that was half that of their MIC. Thus, there is good correlation between the mecillinam suppression activity and the MIC of the A22-like molecules. Because mecillinam suppression activity is reflective of MreB antagonism, this finding is consistent with the activity of A22-like molecules being largely (if not entirely) based on a disruption of Rod system function at concentrations around their MIC.

LolA is unlikely to be a physiologically relevant target for A22-like molecules

The identification of MAC13243 as a potential inhibitor of LolA in the lipoprotein transport pathway (26) and the subsequent finding that this molecule degrades into an A22-like product has led to the suggestion that A22 and its relatives may target LolA as well as MreB (28). On the other hand, the tight correlation between the MIC and mecillinam suppression activity reported here supports a relatively specific mode-of-action for A22-like molecules in targeting MreB. We therefore further investigated the chemical genetic observations connecting

Antimicrobial Agents and Chemotherapy

MAC13243, A22, and LolA. The finding that LolA overproduction suppressed the lethal action of MAC13243 was the initial observation that led to the suggestion that LolA is the target for these molecules (26). It was then later shown that LolA overproduction similarly suppressed killing by A22, suggesting a connection between its activity and lipoprotein transport (28). An alternative interpretation of these results comes from the prior findings that LolA overproduction induces the Rcs envelope stress response (35), and that the Rcs stress response provides resistance to peptidoglycan synthesis inhibitors (21, 36). Thus, we suspected that it is the induction of the Rcs response by *lolA* overexpression that suppresses the lethal activity of A22, not the overproduction of a potential target. To investigate this possibility, we tested the effect of LolA overproduction on A22 lethality in the presence or absence of RcsF, the lipoprotein sensor responsible for triggering the Rcs response (37). As expected based on prior results, LolA overproduction was indeed capable of suppressing cell killing by A22 (**Fig. 5A**). However, this suppressive effect was lost in Δ*rcsF* cells even though similar levels of LolA were produced (**Fig. 5B**), indicating that suppression by LolA overproduction requires the Rcs response.

Rod system inactivation results in an outer membrane permeability defect

MAC13243 was also recently identified in a high-throughput screen for molecules that disrupt the outer membrane permeability barrier of *E. coli* (38). The authors showed that this molecule makes cells more susceptible to bulky antibiotics like vancomycin that are normally excluded by the outer membrane. Given the prior connection of MAC13243 with LolA (26), it was concluded that the permeability defect induced by the compound was a result of its interference with the lipoprotein transport pathway (38). However, based on our analysis above, we reasoned that the observed effect of MAC13243 was more likely to result from its breakdown product inhibiting the Rod system. Accordingly, A22 was previously shown to

sensitize cells to novobiocin, which like vancomycin is normally excluded by the outer membrane (39). To further investigate the effect of MreB inactivation on outer membrane function, we compared the sensitivity of otherwise wild-type FtsZ^{UP} *E. coli* verses a Δ*mreB* derivative growing as spherical cells. The mutant cells were found to be hypersensitive to vancomycin and bile salts (**Fig. 6**). As reported previously, they were also found to be hypersensitive to sodium dodecyl sulfate (SDS) detergent (19) (**Fig. 6**). We therefore conclude that cells inactivated for the Rod system have an outer membrane permeability defect, and that the previously observed effect of MAC13243 on cell permeability is most likely due to its activity against MreB, not LolA.

Other potential Rod system inhibitors and their activity

In addition to A22 (17, 18) and MAC13243 (28, 29) that is hydrolyzed to form an A22-like molecule, there are two additional antagonists of the Rod system of known structure reported in the literature: CBR-4830 (40) and sceptrin (41). The natural product 654/A was recently identified as a possible RodA inhibitor, but its structure has yet to be revealed (42). Of the compounds of known structure, we wondered whether they or their close analogs were present in the chemical library used for screening and if so, why they might not have been identified by the assay procedure.

Sceptrin is a natural product (43) and did not have representation in our library, but similarity analysis identified 66 potential CBR-4830 analogs in the initial library used for the lethality screen (**Table S2**). Of these, 22 inhibited growth and 11 were included in our bioactive sub-library (**Table S2**). None of the 11 CBR-4830 analogs suppressed mecillinam toxicity. To further analyze why these compounds were not identified as hits, we purchased CBR-4830 and analyzed its activity in our growth assays used for screening. Consistent with previous

296 results (40), we found that CBR-4830 inhibited growth of wild-type *E. coli* and induced cell
297 rounding (**Table 1**), suggesting that CBR-4830 may indeed target the Rod system. However,
298 CBR-4830 did not suppress mecillinam toxicity, nor was its inhibitory activity suppressed in
299 FtsZ^{UP} cells (**Table 1**), suggesting that CBR-4830 may have significant off-target activity.
300 Accordingly, CBR-4830 displayed potent lethality against an FtsZ^{UP} strain deleted for the
301 *mreBCD* operon (MIC = 12.5 μg/ml), which was only about four times greater than its MIC
302 against wild-type *E. coli* (3.1 μg/ml). Also, CBR-4830 inhibited the growth of *S. aureus* HG003
303 (MIC = 12.5 μg/mL), a gram-positive bacterium that lacks MreB (**Table 1**). These results are in
304 contrast to the relatively high specificity displayed by A22, which has a ~100-fold reduced
305 potency against Δ*mreBCD* FtsZ^{UP} cells (MIC > 100 μg/mL) relative to wild-type (MIC = 1.6
306 μg/mL), and is inactive against *S. aureus* HG003 (MIC > 100 μg/mL). Thus, we conclude that
307 CBR-4830 has anti-MreB activity in *E. coli*, but has off-target effects that are likely to prevent
308 the suppression of mecillinam toxicity. The potential for similar off-target activity for the CBR-
309 4830 derivatives in our library may also have contributed to their absence among the positive
310 hits from the screen.
311
312
313 **DISCUSSION**
314 In this report, we describe the development and implementation of a high-throughput screen
315 for compounds that disrupt the activity of the Rod system. The screen takes advantage of the
316 conditional essentiality of the complex and the ability of the beta-lactam mecillinam to make its
317 activity toxic (19, 22). These properties allow molecules that promote growth under special
318 circumstances to be identified that are also lethal against wild-type bacteria. Such a screening
319 process has distinct advantages over assays for lethal activity alone because it helps rapidly
320 eliminate non-specific toxins from the set of screening hits. Thus, downstream efforts can be

focused on the characterization of molecules that are on-target and therefore suitable for use as probes for studying cell wall biogenesis and/or use in potential drug development.

The Rod system as an antibiotic target

The Rod system contains several potential drug targets, the most attractive of which are the cell wall synthase enzymes RodA and PBP2 as well as MreB. The other components (MreC, MreD, and RodZ) are also potential targets for antibiotics, but their activities are not well defined. Therefore, the pathway for characterizing and developing molecules active against these proteins is likely to be more difficult than for those hitting the components with activities that can be assayed *in vitro*.

One potential problem with targeting the Rod system is that its essentiality can be relatively easily suppressed by increasing the cellular FtsZ concentration. However, the resulting spheres grow poorly in the laboratory (19) and have outer membrane barrier defects that would sensitize them to a range of insults inside the host. Indeed, coccoid cells of *Shigella flexneri* inactivated for the Rod system also display defects in effector secretion and the ability to invade mammalian cells (44). Thus, the activity of the Rod system is likely to be strictly essential during infection such that the suppression observed in laboratory media is unlikely to be problematic with respect to resistance development in the host. In addition to being attractive targets on their own, RodA and PBP2 have paralogs (FtsW and PBP3) that perform essential roles within the cell division apparatus. Therefore, any molecules identified that target RodA or PBP2 have the potential to also disrupt the activity of FtsW or PBP3, respectively. Such dual targeting activity would be ideal for antibiotic development because it would significantly reduce potential problems with mutational resistance that can cause issues for the development of compounds directed against a single target (45).

An effective screening approach to identify Rod system antagonists

The successful identification of A22-like hits validates the utility of our screening procedure for identifying antagonists of MreB. However, besides this well-studied class of molecules, no additional inhibitor scaffolds targeting MreB or other components of the Rod system were identified. Our previous analysis of mecillinam toxicity found that it could be readily suppressed by the genetic inactivation of any component of the Rod system (22). Therefore, our screen should theoretically be capable of identifying inhibitors of any member of the machinery save for the crosslinking activity of PBP2 that is blocked by mecillinam. Why we only identified A22-like hits targeting MreB in the screen is not known. Although we favor the idea that these results reflect limitations in the chemical space covered by the library used for screening, an unexpected bias of the screen for the identification of MreB antagonists cannot be ruled out without control inhibitors active against other components of the system, of which none are currently known.

The target of A22 and its potential as an antibiotic

A22 has been used as a probe to study MreB and Rod system function for some time (18). The evidence for MreB being its primary target is quite strong, including mutational resistance in the *mreB* gene and structures of MreB with A22 bound near its ATPase active site (18, 25, 29). However, work with the compound MAC13243 has raised questions about the specificity of A22. MAC13243 was originally described as a potential inhibitor of LolA in the lipoprotein transport pathway (26), but was subsequently shown to hydrolyze into an A22-like molecule that is the active component (28). Like MAC13243, LolA overproduction was capable of suppressing A22 lethality and LolA depletion sensitizes cells to A22, suggesting that A22 may also target LolA.

371

372 Although it was reasonable to link MAC13243 and A22 with LolA function based on the
373 chemical genetic observations (26, 28), connections based on gene overexpression and
374 depletion can often be indirect. In this case, LolA overproduction is known to induce the Rcs
375 envelope stress response (35). This observation raised the possibility that it might be the Rcs
376 response that is the underlying cause of the protection from compound treatment as opposed
377 to target overproduction. Consistent with this idea, we show here that induction of the Rcs
378 response is required for A22 resistance in cells overproducing LolA. Sensitization to compound
379 treatment upon protein depletion can be similarly indirect, especially for a factor like LolA that
380 plays a central role in envelope assembly. Thus, the hypersensitivity of LolA-depleted cells to
381 A22, which also targets envelope assembly, does not strongly support LolA targeting by A22.
382 A similar level of synergy was also observed between LolA depletion and the cell wall
383 synthesis inhibitor fosfomycin (28), which targets the precursor synthase MurA, suggesting that
384 LolA depletion is likely to sensitize cells to a number of treatments that disrupt cell wall
385 synthesis. Finally, the available biochemical data also do not provide significant support for
386 LolA targeting as a physiologically relevant mode-of-action for A22. The K_d for the interaction
387 between LolA and A22-like molecules has been measured to be 150-200 μM (28), which is far
388 greater than the 5.9 μM (1.6 μg/ml) MIC of A22. Finally, the ability of A22 to suppress
389 mecillinam toxicity and promote growth would not make sense if it also caused significant
390 defects in the essential lipoprotein targeting pathway. Rather, the tight correlation of MIC and
391 mecillinam suppression activity we observe combined with all of the available genetic and
392 biochemical data indicates that A22-like molecules are relatively specific for MreB.

393

394 Although A22 appears to be quite specific for MreB in bacterial cells and has been a reliable
395 probe for Rod system activity, it has not yet made it to the clinic as an antibacterial therapeutic.

Problems with mammalian cell toxicity (46) as well as with high mutational resistance (2 x 10^{-8} for *P. aeruginosa*) (29) may be the issue. If these liabilities can be overcome, such A22-like derivatives would be attractive leads for future development, either as single agents, or as a component of a combination therapy given that Rod defects sensitize gram-negative bacteria to other antibiotics.

Conclusion

Here, we report a screen for Rod system inhibitors. Although all of the hits identified were A22-like molecules, only one chemical collection was screened. Despite their seemingly large size, the chemical diversity represented in commercial collections is in actuality quite small. Genetic selections for specific missense mutants often yield “hits” at a frequency of 10^{-7}-10^{-9}. Thus, it stands to reason that even when utilizing an effective pathway-directed screen, the likelihood of a 10^{5}- to 10^{6}-member compound library containing even one molecule that answers a specific screen is relatively low. However, given the success of this screening procedure in identifying MreB inhibitors, screens of additional libraries using this assay are worthwhile and have the potential to identify new classes of anti-Rod system compounds that may be useful for antibiotic development.

EXPERIMENTAL PROCEDURES

Media, bacterial strains and plasmids

Cells were grown in lysogeny broth (LB; 1% tryptone, 0.5% yeast extract, 0.5% NaCl ± 1.5% BactoAgar) at 30°C unless indicated otherwise. Antibiotic concentrations used were: Tetracycline (Tet), 5 µg/mL; Ampicillin (Amp), 50 µg/mL; Chloramphenicol (Cam), 25 µg/mL; Kanamycin (Kan), 25 µg/mL. The bacterial strains and plasmids used in this study are listed in Tables S3 and S4, respectively. A description of their construction is included in the Supplementary Text along with a list of the primers used (Table S5). All deletion strains used were obtained from the Keio knockout collection (47) and confirmed by sequencing**.**

We purchased A22 [S-(3,4-Dichlorobenzyl)isothiourea, HCl] from Calbiochem. We purchased **compound 1** (PH000337; 2,4-dichlorobenzyl imidothiocarbamate), **compound 9** (152811; 3,4-Dichlorophenylhydrazine HCl), **compound 11** (T165948; 4-fluorobenzyl imidothiocarbamate HBr, **compound 20** (MP265, PH012544; 4-chlorobenzyle imidothiocarbamate HCl), and **compound 22** (T282057; 2-chlorobenzyl imidothiocarbamate) from Sigma. We purchased **compound 4** (DP01615; 2,4-dichlorobenzyl butylamine) and **compound 21** (S01620, 3-chlorobenzyl imidothiocarbamate) from Maybridge via Fisher Scientific. We purchased **compound 10** (3-(3,4-dichlorophenyl)propan-1-amine), **compound 19** (Z18380660), **compound 23** ([(4-nitrophenyl)methyl]sulfanyl}methanimidamide HCl), and CBR-4830 (EN300-214505) from Enamine. We purchased Sceptrin dihydrochloride (sc-203258) from Santa Cruz Biotechnology. We verified the purchased compounds via LC/MS. All compounds were dissolved in DMSO (J.T.Baker) to 10 mg/mL or the highest obtainable concentration below 10 mg/mL, and stored at -20ºC.

438 **High-throughput screening and hit validation**

439 All screening was conducted at the ICCB-Longwood Screening Facility using 384 well plates
440 (Corning 3701). We performed automated pipetting with a WellMate (Agilent) or Multidrop™
441 Combi (Thermo Fisher), and pin transfer with a customized Epson E2C2515-UL Scara robot
442 paired with an Epson C3-A601S 6-axis robot arm. We screened all compounds in duplicate
443 plates for each condition tested.

444

445 ***E. coli growth inhibition screen:*** Each compound was pin-transferred (300 nl) into 30 µl of
446 LB with 1% NaCl for a final compound concentration of ≈ 25 µM. A mid-log culture of strain
447 NR1099 (23) (30 µl) was then added to achieve a final OD_{600} of 0.0002. Final concentrations of
448 the compounds varied based on the stock concentration of the individual libraries, but typically
449 fell within 6-60 µM (12-30 µg/ml). After incubation at 37ºC for ~23 hrs, the OD_{600} was
450 measured with an EnVision instrument (Perkin Elmer). Wells with an average OD_{600} of less
451 than 0.5 were designated as hits. The data were collated and a preliminary structural analysis
452 performed to eliminate potential PAINS compounds (48). Compounds that were annotated as
453 a known antibiotic (e.g. erythromycin) were also removed from the final hit list. All remaining
454 hits that were commercially-available were purchased as well as close analogs when possible.
455 Note that NR1099 only has a moderate permeability defect under the conditions used for
456 screening. It was found to be roughly 2-3 times as sensitive as its parent strain to novobiocin,
457 moenomycin, aztreonam, trimethoprim, and ciprofloxacin. Its sensitivity to rifampicin was
458 unchanged.

459

460 ***Mecillinam suppression screen:*** MG1655 [WT] with pTB63 [contains *ftsQAZ* operon,
461 pSC101 origin] was grown in LB-Tet overnight at 30ºC. The following morning, the culture was
462 diluted to an OD_{600} of 3.3 x 10^{-6} in LB with added 40 mM $NaNO_3$ to serve as a terminal electron

acceptor and enhance growth in the 384-well plate format where aeration is poor. An aliquot (30 µl) of this culture (equivalent to ~150 cells) was added to all wells of a 384-well plate (Corning, 3701). The bioactive sub-library was then pin transferred to the plates (100 nL of each compound). After incubation at room temperature for ~30 min, 20 µl of LB containing 6.25 µg/mL mecillinam was applied to each well, resulting in a final volume of 50 µl and a final mecillinam concentration of 2.5 µg/mL. As above, final compound concentration varied based on the stock concentration of the individual libraries but typically fell within 2-30 µM (4-10 µg/ml). The plates were incubated for ~72hrs at 30ºC and the OD_{600} was measured. The known Rod inhibitor, A22, was used as a positive control on each plate (final OD_{600} = 0.42 ± 0.02, n = 128), and the compound vehicle, dimethyl sulfoxide (DMSO), was used as the negative control (final OD_{600} = 0.05 ± 0.03, n = 480). Hit criteria required that both replicate values be above a $\bar{x}$ ± 3σ cutoff (OD_{600} ≥ 0.158), which resulted in 72 hits (5.8%). Taking into account technical replicates, we estimate our false positive rate to be ~0.1%.

FtsZ^{UP} suppression screen: Strain JAB063 [Δ*tolC*] containing pTB63 was grown in LB overnight. The resulting culture was then diluted to an OD_{600} of 2 x 10^{-6} the following morning and 50 µl was added to each well. Hit compounds from screen # 2 were then pin transferred (100 nl each) to the wells and the plates were incubated at 30ºC for ~48hrs before measuring the OD_{600}. Hits were identified as those with replicate values above a $\bar{x}$ ± 1σ cutoff (OD_{600} ≥ 0.07), which resulted in 44 hits (61%). This loose cutoff allowed us to cast a wide net for potential rod inhibitors.

Cytological screening

E. coli MG1655 Δ*tolC* [JAB063] was grown to mid-log phase in LB, back-diluted to an OD_{600} of 0.05 and applied to all wells of a 96-well plate (Corning). Potential Rod system inhibitors were

added in a two-fold dilution series with the final concentration ranging from 0.8-25 µg/ml. Cells were then grown with aeration at 30ºC in a VersaMax Microplate Reader with OD_{600} measurements taken every 5min. After treatment for 5hrs, samples at the highest sub-inhibitory concentration were imaged as described previously (49). Morphologies were assessed qualitatively, and those compounds inducing spherical or near spherical cell shape identified as the final set of hits. In addition to the 44 hits identified as putative Rod inhibitors in screen #3, the remaining 28 compounds were also assessed cytologically. All 28 compounds failed to induce cell rounding.

Compound validation

Compounds 1, **4**, **9-11**, **19-24**, CBR-4830 and Sceptrin were purchased (2-100 mg) and validated for growth inhibition via broth microdilution in 96- and 384-well plates (Corning) using the same growth conditions as described for Screen #2. We also validated mecillinam suppression and suppression by $FtsZ^{UP}$ over a range of concentrations (0.2-100 µg/ml) using an HP D300 dispenser for precise titration and a Multidrop™ Combi (Thermo Fisher) for automated pipetting. Bright-field microscopy was performed on wild-type MG1655 cells after treatment with 10-100 µg/ml of compound for 3-4 hrs at 30ºC.

Viability assays

Wild-type *E. coli* MG1655 and Δ*rcsF* [HC397] containing either an empty vector (pHC800) or lolA expression construct (pJAB107) were grown to an OD_{600} of 1.0, serial diluted ten-fold and 5 µl of each dilution spotted onto LB agar containing 0, 1.25, 2.5, 5 or 10 µg/ml A22 in the presence or absence of 500 µM IPTG. Plates were incubated at 30°C for 48hrs and photographed. Similarly, wild-type *E. coli* MG1655 and Δ*mreB* [TU233] expressing $FtsZ^{UP}$ (pTB63) were grown to mid-log phase, diluted to an OD600 of 0.1, serial diluted ten-fold and

spotted onto MacConkey agar or LB agar supplemented with 10 µg/ml of vancomycin, 50 µg/ml of vancomycin, or 1% sodium dodecyl sulfate (SDS). Plates were incubated at 30^{o}C for 48hrs and photographed.

Compound hydrolysis and LC-MS analysis

Stocks of **compounds 4 and 19** were diluted to 500 µM in water with 5% acetonitrile and 0.1% trifluoroacetic acid (TFA). This solution was allowed to sit at room temperature for 0.5 or 18 hr before LC-MS analysis. LC-MS data was collected using an Agilent 6120 Quadrupole LC-MS using electrospray ionization (ESI). LC-MS was conducted with the MS operating in positive ion mode. The compound solutions (5 µL injections) were separated on a Waters Symmetry Shield RP18 column (5 µm, 3.9 x 150 mm) using the following method: flow rate 0.5 mL/min, 95% solvent A (H_2O, 0.1% formic acid) for 5 min followed by a linear gradient of 5% solvent B (acetonitrile, 0.1% formic acid) to 100% B over 15 min.

527 **ACKNOWLEDGEMENTS**

528 The authors would like to thank all members of the Bernhardt, Rudner, Kahne and Walker labs
529 for advice and helpful discussions. We also thank the staff at The Institute for Chemistry and
530 Cell Biology (ICCB-Longwood) Screening Facility at Harvard Medical School for their help in
531 screening and data analysis, and the Microscopy Resources on North Quad (MicRoN) imaging
532 core at Harvard Medical School. This work was supported by the National Institutes of Health
533 (CETR U19 AI109764 to TGB, DK, and SW; F32GM123579 to MAW; F32AI36431 to JFK).

534

REFERENCES

1. **Tacconelli E**, **Carrara E**, **Savoldi A**, **Harbarth S**, **Mendelson M**, **Monnet DL**, **Pulcini C**, **Kahlmeter G**, **Kluytmans J**, **Carmeli Y**, **Ouellette M**, **Outterson K**, **Patel J**, **Cavaleri M**, **Cox EM**, **Houchens CR**, **Grayson ML**, **Hansen P**, **Singh N**, **Theuretzbacher U**, **Magrini N**, **WHO Pathogens Priority List Working Group**. 2018. Discovery, research, and development of new antibiotics: the WHO priority list of antibiotic-resistant bacteria and tuberculosis. Lancet Infect Dis **18**:318–327.

2. **Silver LL**. 2011. Challenges of antibacterial discovery. Clinical Microbiology Reviews **24**:71–109.

3. **Payne DJ**, **Gwynn MN**, **Holmes DJ**, **Pompliano DL**. 2007. Drugs for bad bugs: confronting the challenges of antibacterial discovery. Nat Rev Drug Discov **6**:29–40.

4. **Silver LL**. 2016. A Gestalt approach to Gram-negative entry. Bioorganic & Medicinal Chemistry **24**:6379–6389.

5. **Swoboda JG**, **Meredith TC**, **Campbell J**, **Brown S**, **Suzuki T**, **Bollenbach T**, **Malhowski AJ**, **Kishony R**, **Gilmore MS**, **Walker S**. 2009. Discovery of a small molecule that blocks wall teichoic acid biosynthesis in Staphylococcus aureus. ACS Chem Biol **4**:875–883.

6. **Zhang G**, **Baidin V**, **Pahil KS**, **Moison E**, **Tomasek D**, **Ramadoss NS**, **Chatterjee AK**, **McNamara CW**, **Young TS**, **Schultz PG**, **Meredith TC**, **Kahne D**. 2018. Cell-based screen for discovering lipopolysaccharide biogenesis inhibitors. Proc Natl Acad Sci USA **115**:6834–6839.

556 7. **Brown S**, **Santa Maria JP**, **Walker S**. 2013. Wall teichoic acids of gram-positive
557 bacteria. Annu Rev Microbiol **67**:313–336.

558 8. **Wanner S**, **Schade J**, **Keinhörster D**, **Weller N**, **George SE**, **Kull L**, **Bauer J**, **Grau T**,
559 **Winstel V**, **Stoy H**, **Kretschmer D**, **Kolata J**, **Wolz C**, **Bröker BM**, **Weidenmaier C**.
560 2017. Wall teichoic acids mediate increased virulence in Staphylococcus aureus. Nat
561 Microbiol **2**:16257.

562 9. **Schaefer K**, **Matano LM**, **Qiao Y**, **Kahne D**, **Walker S**. 2017. In vitro reconstitution
563 demonstrates the cell wall ligase activity of LCP proteins. Nat Chem Biol **13**:396–401.

564 10. **Kawai Y**, **Marles-Wright J**, **Cleverley RM**, **Emmins R**, **Ishikawa S**, **Kuwano M**, **Heinz**
565 **N**, **Bui NK**, **Hoyland CN**, **Ogasawara N**, **Lewis RJ**, **Vollmer W**, **Daniel RA**, **Errington**
566 **J**. 2011. A widespread family of bacterial cell wall assembly proteins. The EMBO
567 Journal **30**:4931–4941.

568 11. **D'Elia MA**, **Pereira MP**, **Chung YS**, **Zhao W**, **Chau A**, **Kenney TJ**, **Sulavik MC**, **Black**
569 **TA**, **Brown ED**. 2006. Lesions in teichoic acid biosynthesis in Staphylococcus aureus
570 lead to a lethal gain of function in the otherwise dispensable pathway. Journal of
571 Bacteriology **188**:4183–4189.

572 12. **Shi H**, **Bratton BP**, **Gitai Z**, **Huang KC**. 2018. How to Build a Bacterial Cell: MreB as
573 the Foreman of E. coli Construction. Cell **172**:1294–1305.

574 13. **Typas A**, **Banzhaf M**, **Gross CA**, **Vollmer W**. 2011. From the regulation of
575 peptidoglycan synthesis to bacterial growth and morphology. Nat Rev Micro **10**:123–
576 136.

14. **Meeske AJ**, **Riley EP**, **Robins WP**, **Uehara T**, **Mekalanos JJ**, **Kahne D**, **Walker S**, **Kruse AC**, **Bernhardt T**, **Rudner DZ**. 2016. SEDS proteins are a widespread family of bacterial cell wall polymerases. Nature **537**:634–638.

15. **Cho H**, **Wivagg CN**, **Kapoor M**, **Barry Z**, **Rohs PDA**, **Suh H**, **Marto JA**, **Garner EC**, **Bernhardt T**. 2016. Bacterial cell wall biogenesis is mediated by SEDS and PBP polymerase families functioning semi-autonomously. Nat Microbiol **1**:16172.

16. **Zhao H**, **Patel V**, **Helmann JD**, **Dörr T**. 2017. Don't let sleeping dogmas lie: new views of peptidoglycan synthesis and its regulation. Mol Microbiol **106**:847–860.

17. **Iwai N**, **Nagai K**, **Wachi M**. 2002. Novel S-benzylisothiourea compound that induces spherical cells in Escherichia coli probably by acting on a rod-shape-determining protein(s) other than penicillin-binding protein 2. Biosci Biotechnol Biochem **66**:2658–2662.

18. **Gitai Z**, **Dye NA**, **Reisenauer A**, **Wachi M**, **Shapiro L**. 2005. MreB actin-mediated segregation of a specific region of a bacterial chromosome. Cell **120**:329–341.

19. **Bendezú FO**, **de Boer PA**. 2008. Conditional Lethality, Division Defects, Membrane Involution, and Endocytosis in mre and mrd Shape Mutants of Escherichia coli. Journal of Bacteriology **190**:1792–1811.

20. **Wagstaff J**, **Löwe J**. 2018. Prokaryotic cytoskeletons: protein filaments organizing small cells. Nature Publishing Group **16**:187–201.

21. **Lai GC**, **Cho H**, **Bernhardt T**. 2017. The mecillinam resistome reveals a role for peptidoglycan endopeptidases in stimulating cell wall synthesis in Escherichia coli. PLoS Genet **13**:e1006934.

599 22. **Cho H**, **Uehara T**, **Bernhardt T**. 2014. Beta-lactam antibiotics induce a lethal
600 malfunctioning of the bacterial cell wall synthesis machinery. Cell **159**:1300–1311.

601 23. **Yao Z**, **Davis RM**, **Kishony R**, **Kahne D**, **Ruiz N**. 2012. Regulation of cell size in
602 response to nutrient availability by fatty acid biosynthesis in Escherichia coli. Proc Natl
603 Acad Sci USA **109**:E2561–8.

604 24. **Bean GJ**, **Flickinger ST**, **Westler WM**, **McCully ME**, **Sept D**, **Weibel DB**, **Amann KJ**.
605 2009. A22 disrupts the bacterial actin cytoskeleton by directly binding and inducing a
606 low-affinity state in MreB. Biochemistry **48**:4852–4857.

607 25. **van den Ent F**, **Izoré T**, **Bharat TA**, **Johnson CM**, **Löwe J**. 2014. Bacterial actin MreB
608 forms antiparallel double filaments. Elife **3**:e02634.

609 26. **Pathania R**, **Zlitni S**, **Barker C**, **Das R**, **Gerritsma DA**, **Lebert J**, **Awuah E**, **Melacini**
610 **G**, **Capretta FA**, **Brown ED**. 2009. Chemical genomics in Escherichia coli identifies an
611 inhibitor of bacterial lipoprotein targeting. Nat Chem Biol **5**:849–856.

612 27. **Takacs CN**, **Poggio S**, **Charbon G**, **Pucheault M**, **Vollmer W**, **Jacobs-Wagner C**.
613 2010. MreB drives de novo rod morphogenesis in Caulobacter crescentus via
614 remodeling of the cell wall. Journal of Bacteriology **192**:1671–1684.

615 28. **Barker CA**, **Allison SE**, **Zlitni S**, **Nguyen ND**, **Das R**, **Melacini G**, **Capretta AA**,
616 **Brown ED**. 2013. Degradation of MAC13243 and studies of the interaction of resulting
617 thiourea compounds with the lipoprotein targeting chaperone LolA. Bioorg Med Chem
618 Lett **23**:2426–2431.

29. **Yamachika S**, **Sugihara C**, **Tsuji H**, **Muramatsu Y**, **Kamai Y**, **Yamashita M**. 2012. Anti-Pseudomonas aeruginosa compound, 1,2,3,4-tetrahydro-1,3,5-triazine derivative, exerts its action by primarily targeting MreB. Biol Pharm Bull **35**:1740–1744.

30. **Xia X**, **Maliski EG**, **Gallant P**, **Rogers D**. 2004. Classification of kinase inhibitors using a Bayesian model. J Med Chem **47**:4463–4470.

31. **Rogers D**, **Hahn M**. 2010. Extended-connectivity fingerprints. J Chem Inf Model **50**:742–754.

32. **Iwai N**, **Ebata T**, **Nagura H**, **Kitazume T**, **Nagai K**, **Wachi M**. 2004. Structure-activity relationship of S-benzylisothiourea derivatives to induce spherical cells in Escherichia coli. Biosci Biotechnol Biochem **68**:2265–2269.

33. **Iwai N**, **Fujii T**, **Nagura H**, **Wachi M**, **Kitazume T**. 2007. Structure-activity relationship study of the bacterial actin-like protein MreB inhibitors: effects of substitution of benzyl group in S-benzylisothiourea. Biosci Biotechnol Biochem **71**:246–248.

34. **Nicholson A**, **Perry JD**, **James AL**, **Stanforth SP**, **Carnell S**, **Wilkinson K**, **Anjam Khan CM**, **De Soyza A**, **Gould FK**. 2012. In vitro activity of S-(3,4-dichlorobenzyl)isothiourea hydrochloride and novel structurally related compounds against multidrug-resistant bacteria, including Pseudomonas aeruginosa and Burkholderia cepacia complex. Int J Antimicrob Agents **39**:27–32.

35. **Chen MH**, **Takeda S**, **Yamada H**, **Ishii Y**, **Yamashino T**, **Mizuno T**. 2001. Characterization of the RcsC-->YojN-->RcsB phosphorelay signaling pathway involved in capsular synthesis in Escherichia coli. Biosci Biotechnol Biochem **65**:2364–2367.

640 36. **Laubacher ME**, **Ades SE**. 2008. The Rcs phosphorelay is a cell envelope stress
641 response activated by peptidoglycan stress and contributes to intrinsic antibiotic
642 resistance. Journal of Bacteriology **190**:2065–2074.

643 37. **Cho S-H**, **Szewczyk J**, **Pesavento C**, **Zietek M**, **Banzhaf M**, **Roszczenko P**, **Asmar A**,
644 **Laloux G**, **Hov A-K**, **Leverrier P**, **Van der Henst C**, **Vertommen D**, **Typas A**, **Collet J-**
645 **F**. 2014. Detecting envelope stress by monitoring β-barrel assembly. Cell **159**:1652–
646 1664.

647 38. **Muheim C**, **Götzke H**, **Eriksson AU**, **Lindberg S**, **Lauritsen I**, **Nørholm MHH**, **Daley**
648 **D**. 2017. Increasing the permeability of Escherichia coli using MAC13243. Sci Rep
649 **7**:17629.

650 39. **Taylor PL**, **Rossi L**, **De Pascale G**, **Wright GD**. 2012. A forward chemical screen
651 identifies antibiotic adjuvants in Escherichia coli. ACS Chem Biol **7**:1547–1555.

652 40. **Robertson GT**, **Doyle TB**, **Du Q**, **Duncan L**, **Mdluli KE**, **Lynch AS**. 2007. A Novel
653 indole compound that inhibits Pseudomonas aeruginosa growth by targeting MreB is a
654 substrate for MexAB-OprM. Journal of Bacteriology **189**:6870–6881.

655 41. **Rodríguez AD**, **Lear MJ**, **La Clair JJ**. 2008. Identification of the binding of sceptrin to
656 MreB via a bidirectional affinity protocol. J Am Chem Soc **130**:7256–7258.

657 42. **Emami K**, **Guyet A**, **Kawai Y**, **Devi J**, **Wu LJ**, **Allenby N**, **Daniel RA**, **Errington J**.
658 2017. RodA as the missing glycosyltransferase in Bacillus subtilis and antibiotic
659 discovery for the peptidoglycan polymerase pathway. Nat Microbiol **2**:16253.

660 43. **Walker RP**, **Faulkner DJ**, **Van Engen D**, **Clardy J**. 1981. Sceptrin, an antimicrobial
661 agent from the sponge Agelas sceptrum. J Am Chem Soc **103**:6772–6773.

662 44. **Noguchi N**, **Yanagimoto K**, **Nakaminami H**, **Wakabayashi M**, **Iwai N**, **Wachi M**,
663 **Sasatsu M**. 2008. Anti-infectious effect of S-benzylisothiourea compound A22, which
664 inhibits the actin-like protein, MreB, in Shigella flexneri. Biol Pharm Bull **31**:1327–1332.

665 45. **Silver LL**. 2007. Multi-targeting by monotherapeutic antibacterials. Nat Rev Drug
666 Discov **6**:41–55.

667 46. **van Teeseling MCF**, **de Pedro MA**, **Cava F**. 2017. Determinants of Bacterial
668 Morphology: From Fundamentals to Possibilities for Antimicrobial Targeting. Front
669 Microbio **8**:1264.

670 47. **Baba T**, **Ara T**, **Hasegawa M**, **Takai Y**, **Okumura Y**, **Datsenko KA**, **Tomita M**, **Wanner**
671 **BL**, **Mori H**. 2006. Construction of Escherichia coli K-12 in-frame, single-gene knockout
672 mutants: the Keio collection. Mol Syst Biol **2**.

673 48. **Baell J**, **Walters MA**. 2014. Chemistry: Chemical con artists foil drug discovery. Nature
674 **513**:481–483.

675 49. **Buss JA**, **Peters NT**, **Xiao J**, **Bernhardt T**. 2017. ZapA and ZapB form an FtsZ-
676 independent structure at midcell. Mol Microbiol **104**:652–663.

677 50. **Spratt BG**. 1975. Distinct penicillin binding proteins involved in the division, elongation,
678 and shape of Escherichia coli K12. Proceedings of the National Academy of Sciences
679 **72**:2999–3003.

680 51. **Bendezú FO**, **Hale CA**, **Bernhardt T**, **de Boer PA**. 2009. RodZ (YfgA) is required for
681 proper assembly of the MreB actin cytoskeleton and cell shape in E. coli. The EMBO
682 Journal **28**:193–204.

683

684

685 **FIGURE LEGENDS**

686 **Figure 1. The Rod system and screening rationale**. **A.** Shown is a cartoon of the Rod
687 complex highlighting the individual components. The complex is organized by filaments of
688 MreB. RodA is a PG polymerase that synthesizes the glycan strands of the PG layer (14).
689 PBP2 is a transpeptidase that crosslinks the RodA products into the existing matrix (50). The
690 functions of MreC, MreD, and RodZ remain ill-defined, but RodZ is known to interact directly
691 with MreB (51). **B.** Show is a summary of the genetic properties of Rod system mutants and
692 the response of cells to mecillinam treatment. Note that Rod$^-$ cells with FtsZ^{UP} are resistant to
693 mecillinam (22). This property is the basis of the pathway-directed screen. Molecules that
694 block Rod system activity should rescue growth in the presence of mecillinam.
695
696 **Figure 2. High-throughput screening results**. Shown are scatter plots of OD_{600} readings for
697 cells treated with each test compound in duplicate (Replicate #1 and #2). **A.** The compound
698 collection at the ICCB-Longwood facility was screened for growth inhibition of the outer-
699 membrane defective *E. coli* strain NR1099 (23). Hits were identified as any compound causing
700 the final culture OD_{600} to be less than 0.52 in either replicate. **B.** A sub-library based on the
701 results of screen #1 was assembled and screened for the ability to suppress the toxicity of
702 mecillinam against FtsZ^{UP} cells. Compounds that promoted culture growth to an OD_{600} of 0.158
703 or better ($\bar{x} \pm 3\sigma$) were identified as hits. **C.** Hits from screen #2 were tested for their activity
704 against FtsZ^{UP} cells in the absence of mecillinam. Those that allowed culture growth to an
705 OD_{600} of 0.07 or greater were identified as hits and were considered potential Rod system
706 inhibitors. See text for details. Red dotted lines are the best-fit to the replicate data indicating
707 strong correlation between replicate values. Grey boxes indicate compounds identified as hits.
708 **Figure 3. Effect of selected hits on cell shape.** Phase-contrast micrographs of the efflux-
709 deficient *E. coli* strain MG1655 Δ*tolC* [JAB063] harboring pTB63 [FtsZ^{UP}] after treatment with

0.2% DMSO (**A**), 20 µg/mL of A22 (**B**), ~10 µg/mL of **compound 3** (**C**) or ~10 µg/mL of **compound 7** (**D**) at 30°C for 72 hrs. Scale bar, 5 µm.

Figure 4. Chemical structures of A22 and related hit compounds. A. Chemical structure of A22. **B.** Chemical structures of positive hits from the screening procedure. Green stars highlight hits that were purchased and validated. **C.** Chemical structure of MAC1324 and the products of its hydrolysis. **D.** Chemical structures of A22-like compounds that were negative in the screen for Rod system inhibitors. Red stars highlight true negatives that were purchased and validation. Yellow star highlights the weakly active A22-like molecule that was the lone false negative compound with this scaffold. **E.** Structures of additional A22-like compounds that were purchased for assay validation.

Figure 5. The Rcs response is required for LolA overproduction to suppress A22. A. Cultures of wild-type (WT) *E. coli* MG1655 or a Δ*rcsF* derivative containing plasmid pJAB107 [P_{tac}::*lolA*] were normalized for OD_{600} and dilutions were prepared and spotted onto LB agar with the indicated concentrations of A22 and IPTG. Plates were grown at 30ºC for 48hrs and photographed. **B.** The same strains with either the empty vector control [pHC800] or pJAB107 [P_{tac}::*lolA*] were grown overnight at 30ºC in LB. The resulting cultures were diluted 1:100 and grown at 30ºC to an OD_{600} of 0.2 and as indicated IPTG was added to 500 µM. Growth was continued, and cells from 20 ml of culture were harvested, suspended in 0.5 ml sample buffer, and boiled for 5 minutes. A portion (5 µl) of each extract was run on a 4-20% gradient gel and stained with coomassie brilliant blue. An inducer-dependent band was observed specifically in cells with pJAB107 [P_{tac}::*lolA*] running at the expected molecular weight (MW) of mature LolA (20 kDa). The level of protein produced was unaffected by the *rcsF* mutation.

Antimicrobial Agents and Chemotherapy

735 **Figure 6. Spherical cells have a defective outer membrane permeability barrier.** Spot
736 dilutions across a range of OD_{600} values (1.0 – 1e-5) for wild-type (wt) *E. coli* MG1655 or
737 Δ*mreB* cells harboring pTB63 [$FtsZ^{UP}$] plated onto MacConkey agar containing bile salts, or LB
738 agar containing 10 µg/mL of vancomycin (Vanco), 50 µg/mL of vancomycin, or 1% w/v sodium
739 dodecyl sulfate (SDS). Plates were grown at 30ºC for 48hrs and photographed.

Table 1. Summary of compound activity

				MIC$_{90}$ (ug/mL)[d]					
	inhibit growth[a]	suppress mec[b]	round cells[c]	*E. coli*[e]	*E. coli*[e] + FtsZ^{UP}	Δ*mreBCD*[f] + FtsZ^{UP}	*S. aureus*[g]	min. mec Supp[h]	ratio MIC/mec[i]
A22	+++	Y	Y	1.6	>100	>100	>100	0.8	2
1	+++	Y	Y	0.8	>100	100	100	0.4	2
2	+++	Y	Y	n/a	n/a	n/a	n/a	n/a	n/a
3	+++	Y	Y	n/a	n/a	n/a	n/a	n/a	n/a
4	+++	Y	Y	3.1	>100	>100	100	1.6	2
5	+++	Y	Y	n/a	n/a	n/a	n/a	n/a	n/a
6	+++	Y	Y	n/a	n/a	n/a	n/a	n/a	n/a
7	+++	Y	Y	n/a	n/a	n/a	n/a	n/a	n/a
8	+++	Y	Y	n/a	n/a	n/a	n/a	n/a	n/a
9	+	Y	N	12.5	50	25	12.5	1.6	8
10	+	Y[j]	Y[j,k]	50	>100	50	100	25	2
11	+	Y[j]	Y[j]	12.5	>100	>100	>100	6.25	2
19	+	Y	Y[k]	100	>100	100	>100	50	4
20	+++	Y	Y	1.6	>100	>100	>100	0.8	2
21	+++	Y	Y	6.25	>100	>100	>100	3.1	2
22	+	Y	Y[k]	50	>100	>100	>100	25	2
23	+	Y	Y	50	>100	>100	>100	12.5	4
CBR-4830	+++	ND	Y	3.1	6.25	12.5	12.5	>100	n/a

n/a – not assayed
a: "+++" = strong growth phenotype, OD_{600} reduced > 85%; "+" = weak growth phenotype, OD600 reduced > 40%
b: Results from the high-throughput mecillinam suppression screen using *E. coli* MG1655 + FtsZ^{UP} (pTB63) and a single compound concentration (~10 μM). "Y" = yes, $OD_{600} \geq 0.15$ after 72 hrs at 30°C; "N" = no, $OD_{600} < 0.15$ after 72 hrs at 30°C
c: "Y" = yes, spherical cells observed after treatment with 20 μg/mL; "N" = no, spherical cells never observed
d: Minimum inhibitory concentration (MIC) resulting in 90% reduced growth
e: *E. coli* MG1655 ± FtsZ^{UP} (pTB63)
f: *E. coli* MG1655 Δ*mreBCD* [TU233] FtsZ^{UP} (pTB63)
g: *S. aureus* HG003
h: The minimum compound concentration required to suppress 2.5 μg/mL mecillinam (i.e. $OD_{600} \geq 0.15$ after 72 hrs at 30°C)
i: The ratio of compound MIC_{90} to minimum concentration required for mecillinam suppression
j: Suppression of mecillinam and cell rounding was only observed for the purchased compounds, not the screening aliquots
k: Cell rounding required treatment with 100 μg/mL

A

B

Genotype	[FtsZ]	Drug	Growth	Shape
Rod+	normal	none	+++	Rod
Rod-	normal	none	–	–
Rod-	UP	none	+	Sphere
Rod+	UP	+Mec	–	–
Rod-	UP	+Mec	+	Sphere

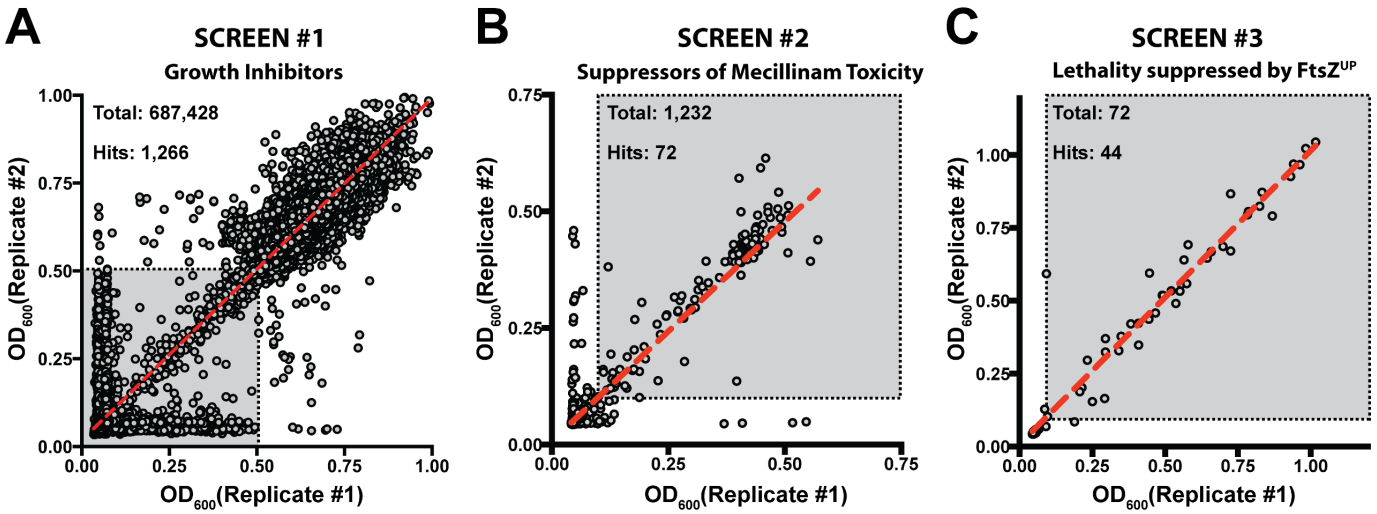

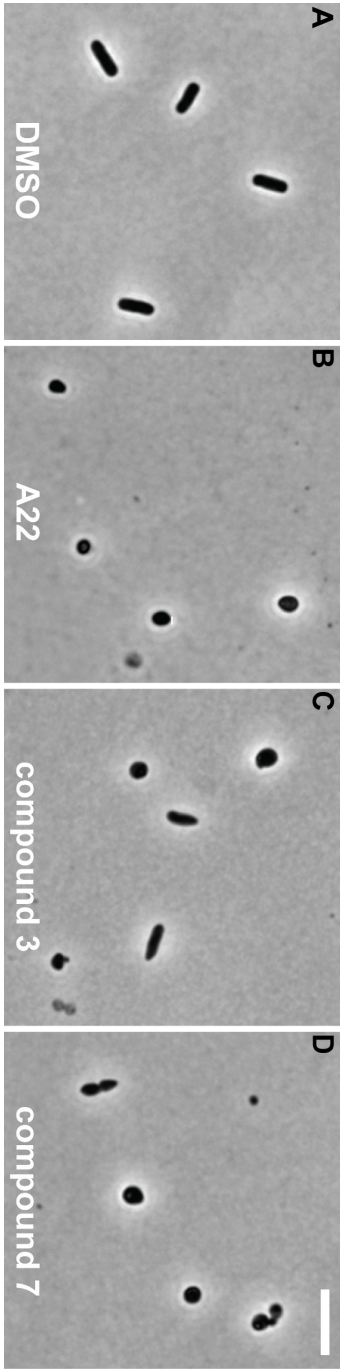

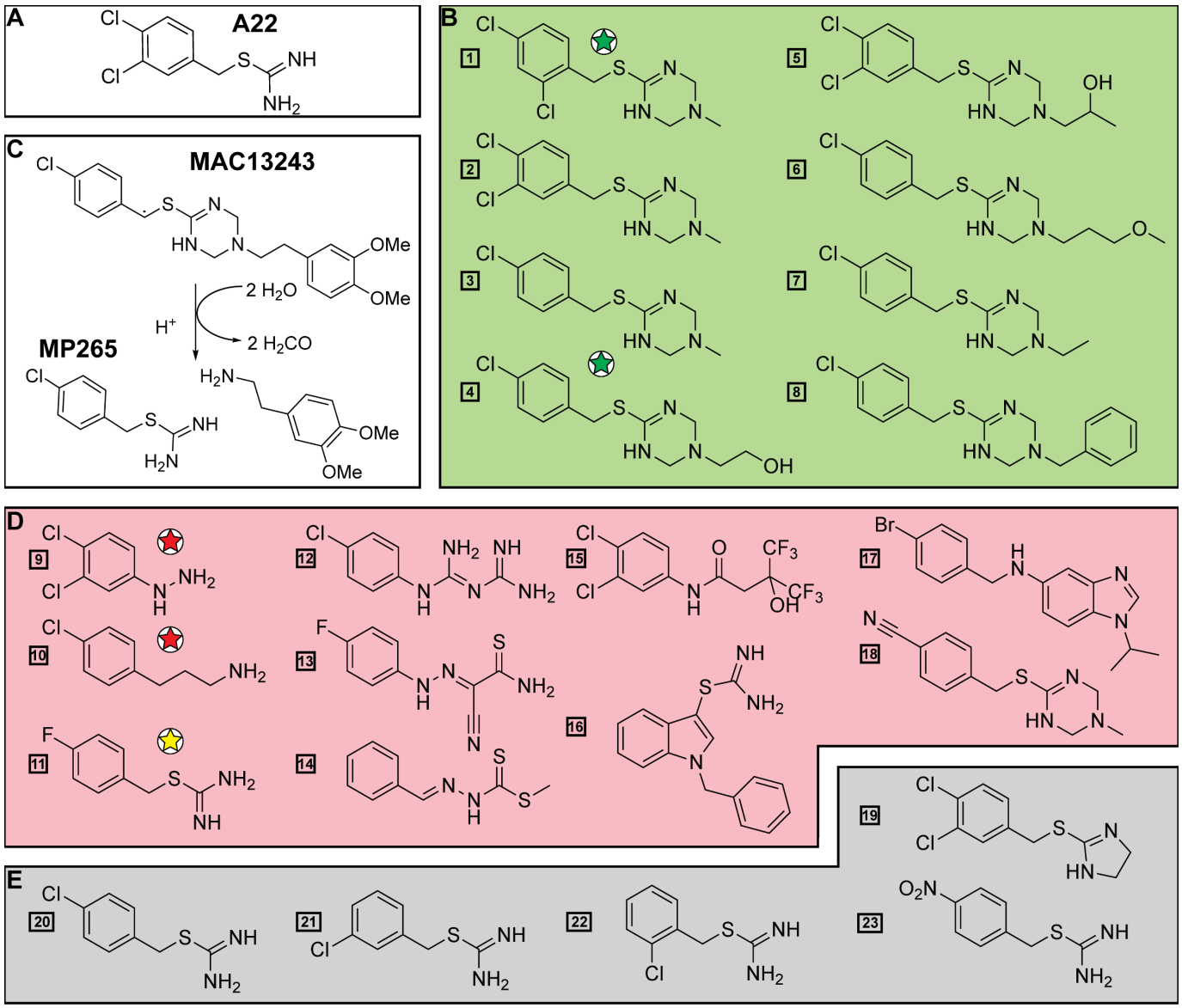

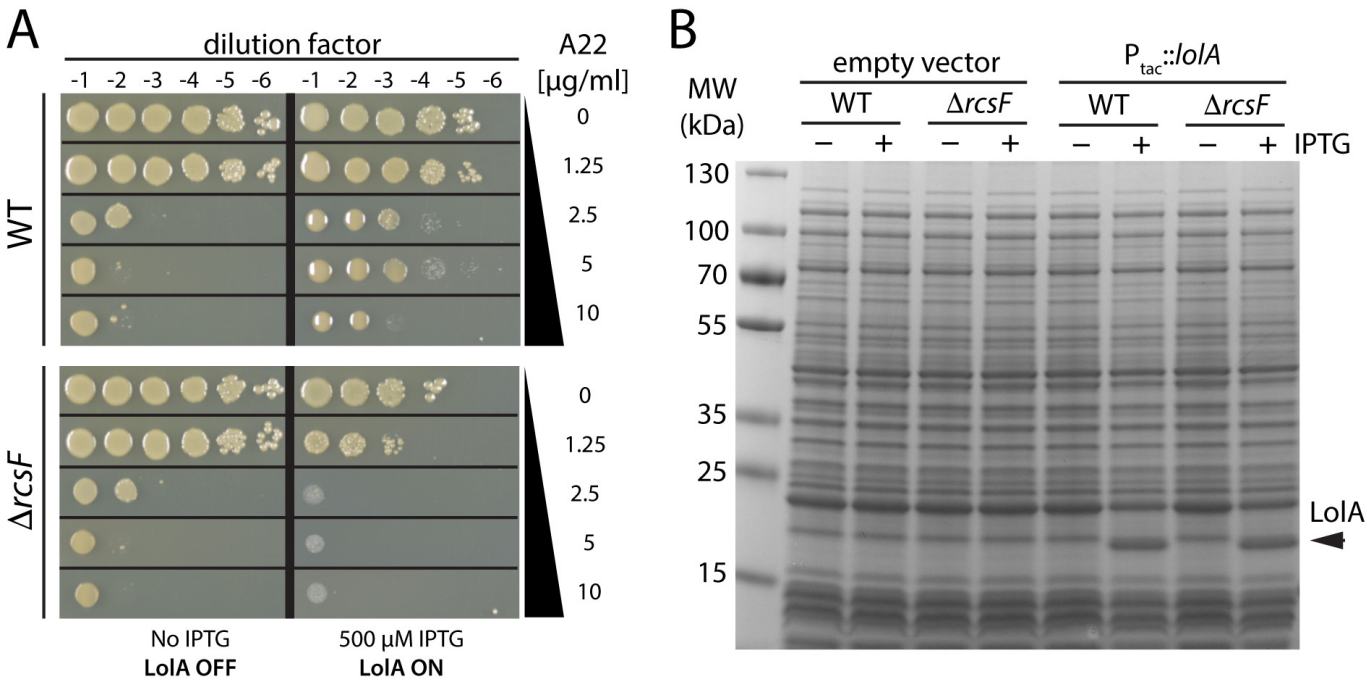

Antimicrobial Agents and Chemotherapy